DFT Investigation of the Tacticity Control during Styrene Polymerization Catalyzed by Single-Component Allyl ansa-Lanthanidocenes {(C5H4CMe2(9-C13H8)}Ln(C3H5)

ARTICLE *in* MACROMOLECULES · AUGUST 2010

Impact Factor: 5.8 · DOI: 10.1021/ma101061r · Source: OAI

DOI: 10.1021/ma101061r

Macromolecules
ARTICLE

DFT Investigation of the Tacticity Control during Styrene Polymerization Catalyzed by Single-Component Allyl *ansa*-Lanthanidocenes $\{(C_5H_4CMe_2(9\text{-}C_{13}H_8)\}Ln(C_3H_5)$

Lionel Perrin,[†] Evgueni Kirillov,[‡] Jean-François Carpentier,*[,‡] and Laurent Maron*[,†]

[†]*LPCNO, UMR 5215, Université de Toulouse-CNRS, INSA, UPS, 135 avenue de Rangueil, 31077 Toulouse Cedex 4, France, and* [‡]*Catalysis and Organometallics, UMR 6226 Sciences Chimiques de Rennes, CNRS-Université de Rennes 1, 35042 Rennes Cedex, France*

Received January 22, 2010; Revised Manuscript Received June 29, 2010

ABSTRACT: Theoretical methods (DFT) were used to investigate the syndiospecificity of the styrene polymerization catalyzed by single-site, single-component allyl *ansa*-lanthanidocenes $\{(C_5H_4CMe_2\text{-}(9\text{-}C_{13}H_8)\}Ln(C_3H_5)$. Two limiting chain-end stereocontrol mechanisms were studied, namely, frontside "migratory" insertion through a site epimerization and site stereoconfiguration independent backside insertion on a "stationary" polymer chain. Four consecutive insertions of styrene were computed to reveal that (i) backside insertions are more favorable than, or at least as favorable as, frontside insertions, and (ii) the formation of a syndiotactic polymer is controlled by the thermodynamics. Moreover, the odd (first and third) insertions are of 2,1-*down-si*-type and are kinetically favored over the 2,1-*up-re*-ones. This control is the conjunction of two effects: minimization of styrene−styrene and styrene(phenyl ring)−fluorenyl repulsions and (iii) the steric hindrance of the polymer chain induces for the fourth insertion an exocyclic coordination of the fluororenyl ligand that is compensated by the η^6 coordination of one the phenyl ring of the growing chain.

Introduction

Syndiotactic polystyrene (sPS) is a potentially attractive material for a number of industrial applications.[1] This inexpensive polymer, which was discovered more than two decades ago, is traditionally available using Ziegler−Natta catalysts.[2,3] Among the latter class, homogeneous binary systems based on mono(cyclopentadienyl)−titanium complexes are the most efficient catalysts.[4] Combinations such as $\{Cp''\}TiX_3$/MAO (Cp'' = substituted cyclopentadienyl, typically C_5Me_5; X = halide, alkoxide, alkyl; MAO = methylaluminoxane) afford large fractions of sPS with high contents of racemic *pentads* (*rrrr* > 90%).[3] In recent years, in line with the extensive search for new-generation polymerization catalysts, a range of highly effective single-site catalyst systems for syndiospecific styrene polymerization has appeared.[4] Of notable importance are systems based on post-metallocene titanium complexes supported by amidinate[5,6] or sulfur-bridged bis(phenolate) ligands,[7,8] as well as metallocene and half-sandwich complexes based on group 3 metals, namely ytterbium,[9] scandium,[10−14] and other lanthanides, especially neodymium,[15,16] some of them featuring very high activity, control over the polymerization and syndiospecificity. In particular, neutral allyl *ansa*-neodymocene complexes of general formula $\{Cp'CMe_2Flu'\}Nd(\eta^3\text{-allyl})(ether)_n$ (Cp' = C_5H_4; Flu' = 9-$C_{13}H_8$; allyl = CH_2CHCH_2; ether = THF, Et_2O, n = 0, 1) reported by some of us are single-component (i.e., they do not require any coactivator) catalysts that operate under industrially relevant conditions (bulk styrene, high temperature).[16] Moreover, with these catalysts, the crude polymers contain neither atactic nor isotactic polystyrene,[17] and, therefore, solvent fractionation is not required to recover pure sPS (*rrrr* > 99%).

*Corresonding authors. E-mail: (J.-F.C.) jean-francois.carpentier@univ-rennes1.fr; (L.M.) laurent.maron@irsamc.ups-tlse.fr.

Our initial experimental investigations allowed us to get only a partial insight into the exact mechanism operative in this neodymocene-catalyzed syndiospecific styrene polymerization. End-groups analyses of low molecular weight sPS by NMR and MALDI−ToF−MS unambiguously showed allyl termini.[16] This indicated that the allyl ligand in the catalyst precursor is the actual initiating group of the polymerization process, but it was not possible at this stage to assess the regioselectivity (1,2- or 2,1-insertion mode) of the first insertion of styrene.[18] Also, in order to identify the origin of the syndiospecificity afforded by these allyl *ansa*-neodymocenes, detailed microstructural analyses were conducted by ^{13}C NMR spectroscopy.[16b] The latter studies showed a perfect match with a Bernoullian statistics, establishing that stereocontrol operates via a chain-end mechanism (CEM). Another experimental observation that supported CEM as the main stereocontrol mechanism was the fact that sPS is still produced using allyl *ansa*-neodymocenes bearing a C_1-symmetric ligand,[19] i.e., $\{(3\text{-}t\text{Bu}C_5H_3)CMe_2(9\text{-}C_{13}H_8)\}Nd(\eta^3\text{-allyl})(THF)$. However, the tacticity of the sPS prepared using such complex was somewhat lower than that of sPS prepared under the same conditions from $\{(C_5H_4)CMe_2(9\text{-}C_{13}H_8)\}Nd(\eta^3\text{-allyl})(THF)$.[16b]

In a recent study, we investigated in details the *initiation* step of styrene polymerization mediated by $\{Cp'CMe_2Flu'\}Ln(\eta^3\text{-allyl})(ether)_n$ complexes.[20] Both experimental (NMR analyses of deuterated sPS produced with such Nd(III) catalysts) and theoretical (DFT computations performed on independently validated Eu(III) analogues; see Experimental Section) approaches demonstrated that 2,1-insertion of styrene is clearly the preferred mode. Moreover, the orientation of the styrene phenyl ring was shown to play an important role in controlling the selectivity of styrene insertions. As expected, DFT computations indicated that orientation of this phenyl ring opposite ("*down*" mode, Chart 1) to the fluorenyl ring (i.e., a more sterically hindered ligand compared

 Published on Web 07/13/2010

Chart 1. Orientation Modes and Nomenclature Used for Styrene Insertion with Respect to the Ancillary Ligand[a]

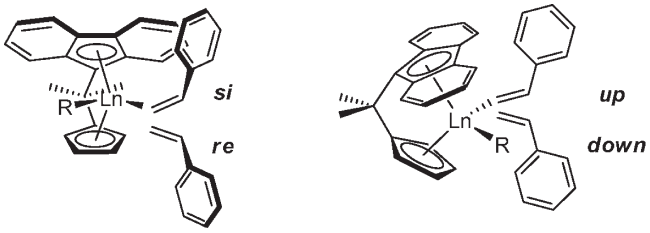

[a] Only one enantiomer of the metal catalyst is depicted, *i.e.*, the one used for "backside" insertions; the opposite enantiomer, *i.e.*, the one involved in the "frontside" insertion, leads to the *up-re* and *down-si* configurations.

to Cp) is the preferred one, both on kinetic and thermodynamic grounds.

Theoretical studies of styrene polymerization propagation steps remain rather scarce in the literature.[21,22] Those computations focused on Ti(III) species using as model geometries ligand−metal frameworks such as [CpTi], [(benzene)Ti] and [*ansa*-Me_2SiCp_2Ti] and were intended at rationalizing the intrinsic role of the chiral orientation of the growing polymeric chain on the regio- (2,1- vs 1,2-insertions) and stereo- (syndiotactic vs isotactic) selectivities of the monomer insertion, as well as stereocontrol mechanisms (CEM vs ECM (enantiomorphic-site control mechanism)). Most of those computations were limited to the second insertion as a model of the propagation step.

The aim of the present contribution on syndiospecific styrene polymerization mediated by {Cp′CMe_2Flu′}Ln(η^3-allyl)(ether)$_n$ complexes was to explore the molecular origin of the CEM that operates in these polymerizations. Thus, both the *propagation* step and its *tacticity* have been studied in details considering 2,1-regioregular insertions and syndiotactic enchainments. Not only the second but also the third and fourth insertions have been computed. In addition, to cover the major chemical events that may occur in the active site of the catalyst, both backside ("stationary")[21,22] and frontside ("migratory") insertions have been considered and investigated.

Results

1. Second Styrene Insertion Reaction. On the basis of the results of our preliminary study on the initiation step of the polymerization reaction mediated by {Cp′CMe_2Flu′}Ln(η^3-allyl)(ether)$_n$ complexes,[20] the second styrene insertion has been computed only from the product (**4*d*-*si***) resulting from a first 2,1-*down* insertion after a *si* coordination of the monomer (Chart 1). This is consistent with previous computations on Ti systems.[21,22] As mentioned in the Introduction, two orientations of the polymer chain have been considered: (i) a backside insertion with a "stationary" polystyryl chain, which corresponds to the coordination of the incoming styrene monomer onto the same coordination site as for the first insertion; (ii) a frontside insertion, which switches the coordination sites of the migratory growing polystyryl chain and of the incoming monomer at each insertion step.

The free energy profiles have been computed for both the 2,1-*up-re* (**6*u*-*re***) and 2,1-*down-si* (**6*d*-*si***) insertions in the first insertion product **4*d*-*si*** (Figure 1). As anticipated, the resulting transition state **6*u*-*re*** is somewhat less stable (by 3.6 kcal mol^{-1}) than **6*d*-*si***, because in the former structure the phenyl styrene ring points toward the fluorenyl ligand (closest C(styrene)···C(fluorenyl) contacts: 3.6−3.7 Å in **6*u*-*re*** vs 4.4−4.5 Å in **6*d*-*si***) (Figure 2). From the kinetic point of view, both barriers ($\Delta_rG^{\circ\#}$ = 31.8−35.4 kcal mol^{-1}) are accessible. These barriers are higher than the one computed for the first

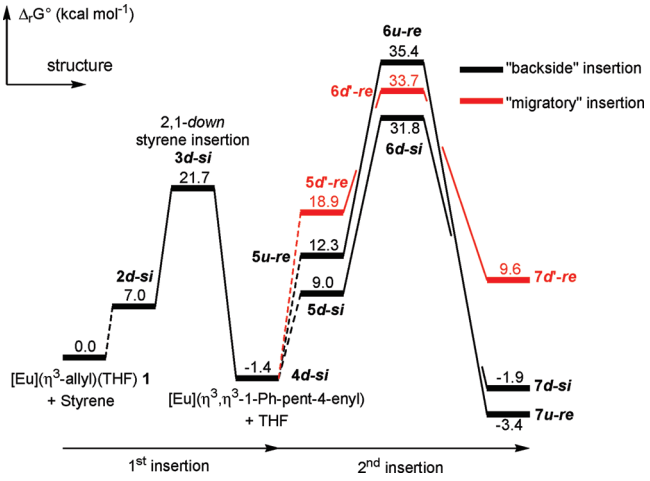

Figure 1. Free enthalpy profiles of the first and second insertions of styrene in {Cp′CMe_2Flu′}Eu(η^3-allyl)(THF) (**1**).

insertion (21.7 kcal mol^{-1} for the 2,1-*down-si* mode (**3*d*-*si***); 28.6 kcal mol^{-1} for the 2,1-*up-re* mode (**3*u*-*re***)).[20] This difference can be explained by further analyzing the geometry of the transition states. In **6*d*-*si*** as well as in **6*u*-*re***, due to the steric hindrance around the metal center, the first inserted styryl group does not interact any more with the metal center in a η^3-fashion but underwent a haptotropic shift toward a reduced η^1-mode; this allows the insertion of the second incoming styrene unit. In contrast, in the styrene adducts **5*d*-*si*** and **5*u*-*re***, the styryl groups remain η^3-coordinated. The double bond of the incoming styrene unit interacts with the metal center in a asymmetrical way; the C^1−Eu distance is shorter than the C^2−Eu one by 0.40−0.50 Å. For the 2,1-*down-si* adduct (**5*d*-*si***), the coordinated styrene is closer to the metal center than in the 2,1-*up-re* adduct (**5*u*-*re***) (C^1−Eu = 2.82 Å vs 3.08 Å and C^2−Eu = 3.35 Å vs 3.62 Å). In adduct **5*u*-*re***, the longer C^2−Eu distance can be explained by the steric repulsion between the phenyl ring of the incoming styrene and the fluorenyl ligand. This results in a slight destabilization of the 2,1-*up-re* adduct (**5*u*-*re***) with respect to 2,1-*down-si* adduct (**5*d*-*si***).

Mechanistically, these structural changes reveal that the coordination−insertion sequence induces the aforementioned haptotropic shift of the first inserted styryl group. Hence, transition states **6*u*-*re*** and **6*d*-*si*** should be better viewed as styrene insertion into a metal−*alkyl* bond rather than in a metal−*allyl* system. Actually, the activation barriers shown in Figure 1 ($\Delta_rG^{\circ\#}$ = 31.8−35.4 kcal mol^{-1}) compare well with the one previously reported for the first 2,1-*down* insertion of styrene into {Cp′CMe_2Flu′}Eu(CH_2SiMe_3)(THF) ($\Delta_rG^{\circ\#}$ = 31.2 kcal mol^{-1}).[20] A similar energetic difference is observed between the *up* and *down* orientation ($\Delta\Delta_rG^{\circ\#}$ = 3.6 kcal mol^{-1} for the second insertion in {Cp′CMe_2Flu′}Eu(η^3-allyl)(THF) vs 4.7 kcal mol^{-1} for the first insertion in {Cp′CMe_2Flu′}Eu(CH_2SiMe_3)(THF)).

Thermodynamically, the 2,1-*up-re* insertion product **7*u*-*re*** is the most stable one, yet the difference of 1.5 kcal mol^{-1} with the 2,1-*down-si* insertion product **7*d*-*si*** is rather small and within the precision of the method. In these two cases, the second insertion is slightly exergonic or almost athermic. This situation is quite similar to the previously studied insertions into an alkyl group, where the reactions were found to be almost athermic (Δ_rG° = 1.0 and 5.9 kcal mol^{-1} for the 2,1-*down* and 2,1-*up* insertion, respectively).[20]

To assess the possible influence of the fluxionality of the growing polymer chain, we investigated the insertion of styrene

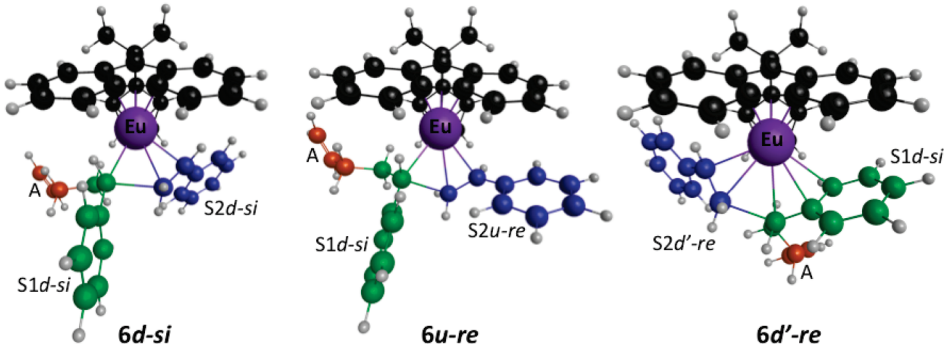

Figure 2. Optimized geometries of the transition states for the second 2,1-insertion of styrene in {Cp′CMe$_2$Flu′}Eu(η^3-allyl)(THF) (**1**). "A" refers to the initial allyl motif, "Sn *d-si*" or "Sn *u-re*" to the *n*th inserted styrene monomer in the *down* or *up*, *si* or *re* configuration, respectively.

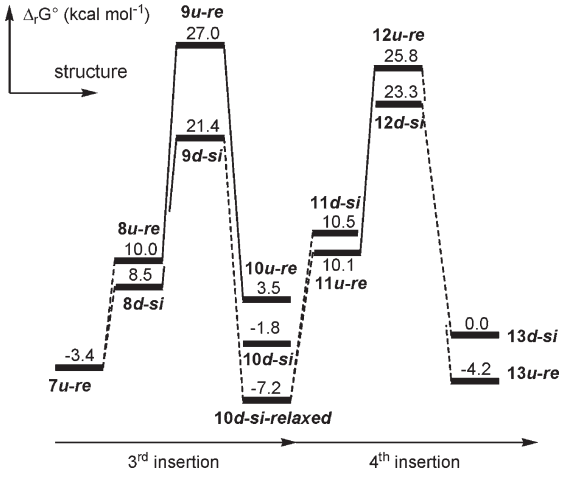

Figure 3. Free enthalpy profile for the third and fourth 2,1-insertions of styrene in {Cp′CMe$_2$Flu′}Eu(η^3-allyl)(THF) (**1**).

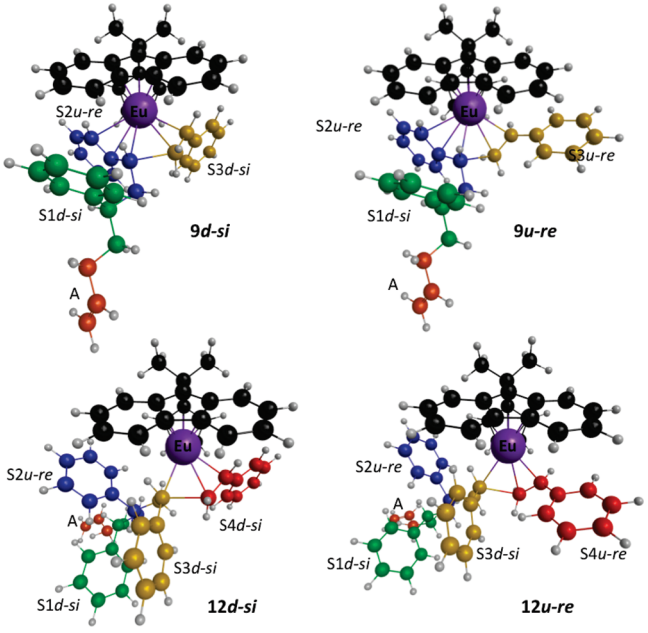

Figure 4. Optimized geometries of the transition states for the third and fourth 2,1-insertion of styrene in {Cp′CMe$_2$Flu′}Eu(η^3-allyl)(THF) (**1**). "A" refers to the initial allyl motif, "Sn *d-si*" or "Sn *u-re*" to the *n*th inserted styrene monomer in the *down* or *up*, *re* or *si* configuration, respectively.

via an alternative coordination site; that is, after switching the chain coordination site, as usually considered for α-olefin polymerization via migratory insertion (**5*d′-re***, **6*d′-re***, and **7*d′-re*** in Figures 1 and 2). An activation barrier of 33.7 kcal mol^{-1} was calculated in this case, which is very similar to the ones computed for the backside styrene insertions. It is noteworthy that the insertion products **7*u-re*** and **7*d′-re***, which result respectively from the 2,1-*up-re* backside (**6*u-re***) and 2,1-*down-re* frontside (**6*d′-re***) transition states, are diastereomeric in nature, formally differing by the absolute configuration at the metal center. However, some differences are noted in the computed products. Indeed, product **7*u-re*** is an allyl compound, whereas product **7*d′-re*** is best described as an alkyl compound (see Figure S1, Supporting Information). As a result, the latter insertion reaction is endergonic by ca. 10 kcal mol^{-1}. Note that the formation of an alkyl compound in styrene polymerization was already reported to be endergonic by 8−10 kcal mol^{-1}.[21] Hence, there is no significant energy gain to proceed according to this frontside migratory insertion scheme and therefore, in the following, only propagation via backside attack will be considered, in agreement with previous studies on titanium-based systems.[21,22]

2. Third Styrene Insertion Reaction. As we did for the second insertion, only third styrene insertions starting from the most stable product of the previous (second) insertion were considered, that is from the 2,1-*up-re* second insertion product (**7*u-re***). The free energy profile computed for the third insertion is shown in Figure 3.

The 2,1-*down-si* insertion leads to transition state **9*d-si*** with an activation barrier of 21.4 kcal mol^{-1}, which is very similar to the analogous one found for the first insertion leading to **3*d-si*** ($\Delta_r G^{\circ\#}$ = 21.7 kcal mol^{-1}; Figure 1).[20] Reversely, the third 2,1-*up-re* insertion leads to transition state **9*u-re*** and operates with a higher barrier (as compared to **9*d-si***), with an energy difference of 5.6 kcal mol^{-1}. Again, the latter value is very similar to the energetic difference observed between the transitions states **3*d-si***/**3*u-re*** for the first insertion (6.9 kcal mol^{-1}). These trends can be understood on the basis of structural similarities between transition states **3*d-si***/**9*d-si*** and **3*u-re***/**9*u-re***, respectively. Indeed, in **9*d-si*** (Figure 4), the last inserted styryl unit still interacts with the metal center in a η^3 fashion (range of Eu−C(styryl) bond distances, 2.81−2.86 Å), which is similar to what observed in **3*d-si*** (range of Eu−C(styryl) bond distances, 2.72−2.88 Å) and in the starting allyl (C_3H_5) complex **1** (range of Eu−C(allyl) bond distances, 2.66−2.69 Å). This bonding interpretation matches the electronic population analysis (NBO) that indicates that the charges of the styryl coordinated carbon atoms [*ortho* (−0.40), *ipso* (−0.13), and CH_2 (−0.45)] in **9*d-si*** are similar to those found for the allyl (C_3H_5) moiety in precursor **1** (−0.42, −0.13, −0.43, respectively). Transition state **9*u-re*** appears destabilized relatively

to **3*d-si***/**9*d-si*** because of the significant repulsive interactions between the phenyl ring of the coordinated styrene monomer unit and the fluorenyl ligand, as previously observed for the first insertion.

Thermodynamically, the 2,1-*down-si* insertion product **10*d-si*** is the most stable one, although the reaction was found to be almost athermic considering the precision of the method. This is due to the geometric constraint of the polymer chain in product **10*d-si*** that originates from the intrinsic reaction coordinate following of transition state **9*d-si***. Indeed, further relaxing the geometry of the polymer chain led to a stabilization of 5.4 kcal mol^{-1} of the complex ("**10*d-si-relaxed***", Figure 3; see Figure S2, Supporting Information).

3. Fourth Styrene Insertion Reaction. For the fourth insertion, we again considered only the most stable product of the third 2,1- backside insertion (**10*d-si***). This choice is even more reasonable considering the very large energetic difference between transition states **9*d-si*** and **9*u-re*** that makes **10*u-re*** an irrelevant (i.e., of negligible impact) intermediate in terms of catalysis. The free energy profile computed for the fourth insertion (Figure 4) is quite similar to the one calculated for the second insertion (Figure 1). The structure of transition states **12*u-re*** and **12*d-si*** are very similar to those optimized for the second insertion (**6*u-re*** and **6*d-si***, respectively; Figures 2 and 4). In particular, the last inserted styryl moiety in **12*u-re*** interacts with the metal center in a η^1 fashion, whereas the incoming styrene unit interacts in a η^2 mode, and the corresponding Eu−C bond distances are similar to those observed in **6*u-re*** (Eu−*C* = 2.73, and 2.59, 2.82 Å in **12*u-re*** *vs* 2.69, and 2.60, 2.79 Å in **6*u-re***, respectively). The activation barriers for the 2,1-*up* (**12*u-re***) and 2,1-*down* (**12*d-si***) fourth insertions are very close to each other ($\Delta_r G^{\circ\#}$ = 25.8 and 23.3 kcal mol^{-1}, respectively). Because of structural similarities between second and fourth insertion transition states, the energetic difference for the barriers in the second (3.6 kcal mol^{-1}) and fourth (2.5 kcal mol^{-1}) insertions are also very similar. Thus, as for the second insertion (**6*u-re***), this fourth insertion can be better described as a styrene insertion into an Ln−*alkyl* bond.

Thermodynamically, the 2,1-*up* insertion product **13*u-re*** is the most stable one, with a slight exergonicity of 4.2 kcal mol^{-1}, while the 2,1-*down* insertion leading to product **13*d-si*** is athermic. This difference may result from the stabilizing interaction between the phenyl ring of the *pre*-inserted styrene unit and the metal center in **13*u-re***. Indeed, the Eu−C_{Ph} distances lie in a quite short-range of 2.97−3.03 Å, evidencing a strong coordination of η^6-type.[23] At the same time, another remarkable peculiarity of **13*u-re*** is the reduced and exocyclic coordination of the fluorenyl moiety. No such interactions between phenyl rings of the polystyryl chain and the metal center nor similar exocyclic coordination/reduced hapticity of the fluorenyl ligand were observed in any other structures computed in this study. This point is further discussed in the subsequent section.

Discussion

1. Periodicity of the Insertion Reactions. The above results show that insertions occur on a "stationary" growing polymer chain via a backside insertion mechanism. The results revealed also sequential/periodic trends in these insertion reactions, both at the transitions states (kinetics) and insertion products (thermodynamics).

For the first and third insertions, the 2,1-*down-si* insertions are found to be kinetically and thermodynamically the most favorable reactions. It is noteworthy that the nature of the corresponding transition states, **3*d-si*** and **9*d-si***, is very similar in terms of geometry. In particular, the polystyryl chain interacts with the metal center in a η^3 coordination mode in both cases. This can be explained by the fact that the *si* orientation of the incoming styrene unit minimizes the repulsive interaction with the six-membered ring of the fluorenyl ligand. Although **3*u-re*** and **9*u-re*** are higher in energy than **3*d-si*** and **9*d-si***, it is noticeable that the former transition states have also a geometry quite similar to each other.

For the second and fourth insertions, the 2,1-*up-re* and 2,1-*down-si* insertions are kinetically comparable; yet, the 2,1-*up-re* insertions are thermodynamically the most favorable. The geometry of the corresponding transition states, **6*u-re*** and **12*u-re***, are very similar. In particular, due to the steric repulsion between the incoming styrene and the six-membered ring of the fluorenyl, the polystyryl chain at the transition state interacts with the metal center in a η^1 mode, that is, similar to a regular alkyl group. Thus, the corresponding activation barriers are higher, which is in line with the results found in a previous study when insertion of styrene into a Y−alkyl bond was studied.[20] Also, the geometries of transition states **6*d-si*** and **12*d-si*** are almost identical.

Similar sequential/periodic trends are observed for the insertion products. The geometries of the first and third insertions, **4*d-si*** and **10*d-si*** (also of **4*u-re*** and **10*u-re***), and of the second and fourth insertions, **7*d-si*** and **13*d-si***, are very close to each other, respectively. The only peculiarity is observed for the fourth insertion product, **13*u-re***, which features an exocyclic coordination of the fluorenyl ligand with reduced hapticity, in contrast to the second insertion product **7*u-re*** (Figure 5). Apparently, this exocyclic coordination in **13*u-re*** finds its origin in the steric repulsion between the incoming styrene and the six-membered ring of the fluorenyl ligand. This coordination change does not occur in the case of complex **7*u-re*** because the growing polymer chain is not long/bulky enough to maximize the steric repulsion (a **13*u-re***-like complex of **7*u-re*** was optimized and found to be less stable by 4.1 kcal mol^{-1}). The reduced coordination mode of the fluorenyl ligand in **13*u-re*** is counterbalanced by an interaction between a phenyl ring of the polystyryl chain and the metal center; a second order perturbation NBO analysis indicates a 25 kcal mol^{-1} interaction.

The fact that the fluorenyl ligand can adopt several exocyclic coordination modes, leading to stable complexes, was already reported in the literature. For instance, crystal structures of early transition metals complexes exhibiting η^3 (η^2) exocyclic coordination modes of the fluorenyl ligand are described for Y, La[24] and Zr.[25] Moreover, reversible haptotropic slippage of a fluorenyl ligand, i.e., η^6 (C_6-*endocyclic*) ↔ η^3(or η^4) (C_6-*exocyclic*) ↔ η^5 (C_5-*endocyclic*) metal migration process, in (Cp)M(η^n-Flu) complexes of Fe and Ru was investigated by experimental and DFT methods.[26] In the context of the current study, it is noteworthy that such dynamic phenomena that lead to changes in the coordination mode of the fluorenyl ligand were proposed to be a key factor accounting for the high catalytic performance of early transition metal (especially, group 4) fluorenyl complexes in α-olefin polymerization.[19b,27] In these studies by Razavi, Alt, and Samuel, it was hypothesized that the fluorenyl ligand, thanks to its rich π-electron system and its various fluxional coordination modes, can effect minute (temporary) stabilization of the electronic configuration and geometry of active species at different stages of the catalytic process. Our computations suggest that these fluxional phenomena are

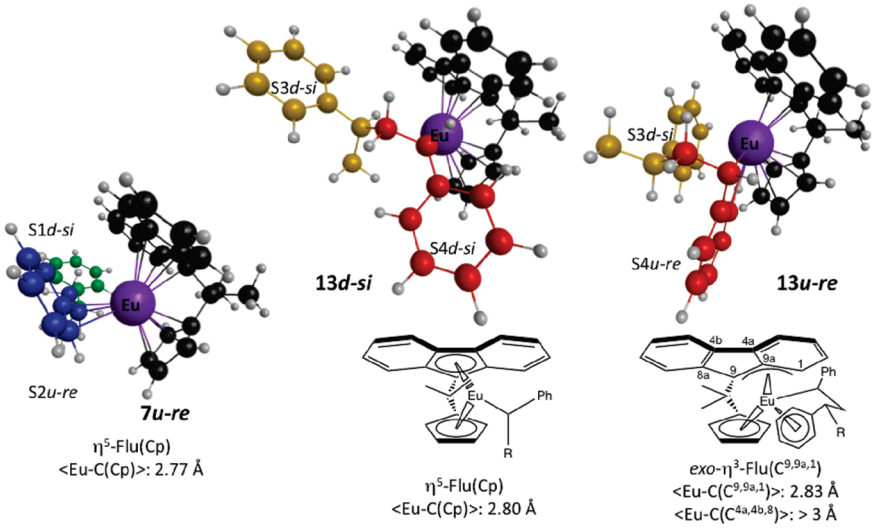

Figure 5. Optimized geometries of insertion products **7*u-re***, **13*d-si*** and **13*u-re***, and idealized representations with main bond distances. "Sn *d-si*" or "Sn *u-re*" refers to the *n*th inserted styrene monomer in the *down* or *up*, *re* or *si* configuration, respectively. The first and second styrene units in **13*d-si*** and **13*u-re*** have been removed for clarity.

also likely relevant to styrene polymerization mediated by Ln−fluorenyl catalysts.

2. Origin of Syndiospecificity. Chain-end control mechanism (CEM), in which the last styrene unit inserted in the growing polymer chain governs the chirality of the next incoming styrene monomer, is the stereocontrol mechanism that is generally accepted for syndiospecific polymerization of styrene mediated by titanium-based catalysts.[21,22] CEM is also known to be operative for alkalino-earth and rare-earth catalysts that are highly effective for the synthesis of syndiotactic polystyrene.[4,9,10] As mentioned in the Introduction, several experimental observations unambiguously support such a stereocontrol mechanism with the $\{(C_5H_4CMe_2(9\text{-}C_{13}H_8)\}Ln(C_3H_5)$ catalysts.[16] The main objective of this study was to investigate in more detail this stereocontrol process.

In order to produce a syndiotactic polymer, there must necessary be an alternation/inversion and *only one*, either in the coordination mode (enantioface) of the styrene monomer *or* in the absolute configuration at the metal center (via migration of the polystyryl chain, *i.e.*, epimerization). For instance, at the second insertion stage (considering that the first one proceeded in a 2,1-*down* backside fashion, leading to a *si* inserted styrene unit), a syndiotactic enchainment can be achieved in principle either by a 2,1-*up* backside insertion or a 2,1-*down* frontside insertion. At this stage, the conclusions drawn from our calculations are limited to the fact that the backside insertion is clearly favored over the frontside insertion. Indeed, all the second insertions were computed to proceed with a similar activation barrier (within the intrinsic precision of the method) and only a slight thermodynamic preference for the 2,1-*up* backside insertion is observed. To gain a better insight into the tacticity, it is necessary to go further on the propagation process.

For the third insertion, the 2,1-*down* backside insertion is found to be significantly thermodynamically and kinetically favorable, leading to the formation of a syndiotactic unit. Thus, up to the third insertion, the formation of a syndiotactic sequence is thermodynamically favored over the formation of isotactic or atactic sequences. For the first and third insertions, the 2,1-*down* insertion is also kinetically favored. For the fourth backside insertion, the thermodynamic preference for the 2,1-*up* over the 2,1-*down* appears to be more pronounced ($\Delta\Delta_rG° = 4.2$ kcal mol^{-1}) than for the second one ($\Delta\Delta_rG° = 1.5$ kcal mol^{-1}), whereas the activation barrier are once again found comparable. Further computations up to sixth insertion would be required to evaluate if this difference is really meaningful, although this is currently hardly manageable considering the large size of these systems.

Overall, the results of those computations suggest that the formation of a syndiotactic polymer is thermodynamically controlled. This is a superposition of two effects. The first one is the classical minimization of the phenyl−phenyl interaction between two styrene units with the growing polymer chain. The second one is the minimization of the repulsion between the incoming styrene unit and the six-membered ring of the fluorenyl ligand. This is obvious when styrene inserts in a *down* mode, i.e., for the first and third insertions; for the second and fourth insertions which proceed in a *up* mode, the incoming styrene orientates its phenyl ring away from the fluorenyl moiety to minimize contacts. Moreover, these results show that, after the first styrene insertion, the metal retains its absolute configuration over the polymerization course; that is, there is no migration of the growing polymer chain, i.e., no epimerization, during the growth a given polymer chain. The systematic alternated *down*/*up* orientation [that is, the reversal in the coordination mode/enantioface] of the monomer at each insertion step appears to be a direct consequence of the configuration of the last inserted monomer unit.

Conclusions

In this study, the factors controlling the formation of syndiotactic polystyrene by $\{C_5H_4CMe_2(9\text{-}C_{13}H_8)\}LnR$ catalysts have been investigated by theoretical methods. By determining the four first insertions, it has been possible to show the following: (1) backside insertions on a "stationary" polymer chain (i.e., no change of coordination site between two insertions) are more favorable than, or at least as favorable as, frontside "migratory" insertions. (2) The formation of a syndiotactic polymer is controlled by the thermodynamics. Moreover, the odd (first and third) insertions are of 2,1-*down*-type and are kinetically favored over the 2,1-*up*-ones. This control is the conjunction of two effects, namely the minimization of the styrene−styrene repulsion as well as styrene(phenyl ring)-fluorenyl ones. (3) The steric hindrance of the polymer chain induces for the fourth insertion

an exocyclic coordination of the fluorenyl ligand that is compensated by the η^6 coordination of one of the phenyl ring in the growing chain.

Experimental Section

Computational Details. The calculations were carried out on europium compounds, due to a technical program of gaussian03 that cannot handle easily f-in-core RECP with an even number of core electrons (e.g., Nd). Previous studies on the lanthanides series[28] have shown that there is very little difference on the reactivity between Nd, Sm, or Eu, especially when dealing with thermodynamic data.

Europium was represented with a Stuttgart−Dresden pseudopotential that includes the 4f electrons in core in combination with its adapted basis set.[29] The basis set has been augmented by the f function (α = 1.0). Carbon and hydrogen atoms have been described with all electrons 6-31G(d,p) double−ζ quality basis sets.[30] Calculations were carried out at the DFT level of theory using the hybrid functional B3PW91.[31] Geometry optimizations were carried out without any symmetry restrictions; the nature of the *extrema* (*minima* and transition states) was verified with analytical frequency calculations. Connectivity of each transition state was determined while following their intrinsic reaction coordinates (IRC). All the computations were performed with the Gaussian 03 suite of programs.[32] The electronic density was analyzed according to the Natural Population Analysis (NPA) scheme.[33] The NBO analysis[33] on a europium complex was carried out using the technique proposed by Clark et al.[34]

Acknowledgment. We are grateful to the CNRS and UPS for financial support of this work. CalMip (CNRS, Toulouse, France) is acknowledged for calculation facilities. J.-F.C. and L.M. thank the Institut Universitaire de France.

Supporting Information Available: Figures S1 and S2, showing optimized structures, and a table giving Cartesian coordinates for the all the optimized structures (complexes, adducts, and transition states). This material is available free of charge via the Internet at http://pubs.acs.org.

References and Notes

(1) Malanga, M. *Adv. Mater.* **2000**, *12*, 1869.
(2) Ishihara, N.; Kuramoto, M.; Uoi, M. (to Idemitsu Kosan Co Ltd) *Jap. Pat.* 62,187,708, 1985.
(3) Ishihara, N.; Seimiya, T.; Kuramoto, M.; Uoi, M. *Macromolecules* **1986**, *19*, 2464.
(4) (a) Rodrigues, A.-S.; Kirillov, E.; Carpentier, J.-F. *Coord. Chem. Rev.* **2008**, *252*, 2115. (b) Schellenberg, J. *Prog. Polym. Sci.* **2009**, *34*, 688.
(5) (a) Flores, J. C.; Chien, J. C. W.; Rausch, M. D. *Organometallics* **1995**, *14*, 1927. (b) Flores, J. C.; Chien, J. C. W.; Rausch, M. D. *Organometallics* **1995**, *14*, 2106.
(6) (a) Liguori, D.; Grisi, F.; Sessa, I.; Zambelli, A. *Macromol. Chem. Phys.* **2003**, *204*, 164. (b) Liguori, D.; Centore, R.; Tuzi, A.; Grisi, F.; Sessa, I.; Zambelli, A. *Macromolecules* **2003**, *36*, 5451.
(7) (a) Capacchione, C.; Proto, A.; Ebeling, H.; Mülhaupt, R.; Moller, K.; Spaniol, T. P.; Okuda, J. *J. Am. Chem. Soc.* **2003**, *125*, 4964. (b) Capacchione, C.; Manivannan, R.; Barone, M.; Beckerle, K.; Centore, R.; Oliva, L.; Proto, A.; Tuzi, A.; Spaniol, T. P.; Okuda, J. *Organometallics* **2005**, *24*, 2971. (c) Beckerle, K.; Manivannan, R.; Lian, B.; Meppelder, G.-J. M.; Raabe, G.; Spaniol, T. P.; Ebeling, H.; Pelascini, F.; Mülhaupt, R.; Okuda, J. *Angew. Chem., Int. Ed.* **2007**, *46*, 4790. (d) Carpentier, J.-F. *Angew. Chem., Int. Ed.* **2007**, *46*, 6404.
(8) (a) Kim, Y.; Hong, E.; Lee, M. H.; Kim, J.; Han, Y.; Do, Y. *Organometallics* **1999**, *18*, 36. (b) Kim, Y.; Han, Y.; Hwang, J.-W.; Kim, M. W.; Do, Y. *Organometallics* **2002**, *21*, 1127.
(9) Harder, S. *Angew. Chem., Int. Ed.* **2004**, *43*, 2714.
(10) Luo, Y.; Baldamus, J.; Hou, Z. *J. Am. Chem. Soc.* **2004**, *126*, 13910.
(11) Hitzbleck, J.; Beckerle, K.; Okuda, J.; Halbach, T.; Mülhaupt, R. *Macromol. Symp.* **2006**, *236*, 23.
(12) Jaroschik, F.; Shima, T.; Li, X.; Mori, K.; Ricard, L.; Le Goff, X.-F.; Nief, F.; Hou, Z. *Organometallics* **2007**, *26*, 5654.
(13) Fang, X.; Li, X.; Hou, Z.; Assoud, J.; Zhao, R. *Organometallics* **2009**, *28*, 517.
(14) Bonnet, F.; Da Costa Violante, C.; Roussel, P.; Mortreux, A.; Visseaux, M. *Chem. Commun.* **2009**, 3380.
(15) Zinck, P.; Valente, A.; Mortreux, A.; Visseaux, M. *Polymer* **2007**, *48*, 4609.
(16) (a) Kirillov, E.; Lehmann, C. W.; Razavi, A.; Carpentier, J.-F. *J. Am. Chem. Soc.* **2004**, *126*, 12240. (b) Rodrigues, A.-S.; Kirillov, E.; Lehmann, C. W.; Roisnel, T.; Vuillemin, B.; Razavi, A.; Carpentier, J.-F. *Chem.−Eur. J.* **2007**, *13*, 5548.
(17) Replacing the Cp′CMe_2Flu′ ligand by a CMe_2(9-Indenyl)$_2$ ligand led to racemic C_2-symmetric complexes that are perfectly isospecific single-site catalysts for styrene polymerization; see: Rodrigues, A.-S.; Kirillov, E.; Roisnel, T.; Razavi, A.; Vuillemin, B.; Carpentier, J.-F. *Angew. Chem., Int. Ed.* **2007**, *46*, 7240.
(18) Contrasted observations have been made for the regioselectivity of styrene insertion with group 3 metal catalysts.[4] (a) Bercaw et al. reported a first 1,2-insertion of styrene with the scandium hydrido complex [Sc(η^5:η^1-$C_5Me_4SiMe_2NCMe_3$)(μ-H)(PMe_3)]$_2$, followed by a 2,1-insertion to yield [Sc(η^5:η^1-$C_5Me_4SiMe_2NCMe_3$)(CH(Ph)$CH_2CH_2CH_2$Ph)(PMe_3)]: Shapiro, P. J.; Schaefer, W. P.; Labinger, J. A.; Bercaw, J. E.; Cotter, W. D. *J. Am. Chem. Soc.* **1994**, *116*, 4623. (b) Teuben et al. reported catalytic dimerization of styrene utilizing lanthanidocene hydrides to give preferably the tail-to-tail coupled product trans-1,4-diphenylbut-1-ene: Kretschmer, W. P.; Troyanov, S. I.; Meetsma, A.; Hessen, B.; Teuben, J. H. *Organometallics* **1998**, *17*, 284. (c) Conversely, Okuda et al. observed exclusive (and irreversible) 2,1-insertion of styrene with the dimeric hydrido complex [Y(η^5:η^1-$C_5Me_4SiMe_2NCMe_3$)(μ-H)(THF)]$_2$: Hultzsch, K. C.; Voth, P.; Beckerle, K.; Spaniol, T. P.; Okuda, J. *Organometallics* **2000**, *19*, 228. (d) The latter observation is consistent with DFT studies for titanocene catalysts which showed that primary insertion is favored in the initiation step but leads to a stable product that blocks additional primary insertions, thus favoring secondary insertion in the propagation step.[21,22]
(19) In polymerization of α-olefins catalyzed by group 4 metallocenes, the C_1-symmetry precursors produce highly isotactic polymers via enantiomorphic site control mechanism. See: (a) Razavi, A.; Bellia, V.; De Brauwer, Y.; Hortmann, K.; Peters, L.; Sirol, S.; Van Belle, S.; Thewalt, U. *Macromol. Chem. Phys.* **2004**, *205*, 347. (b) Razavi, A.; Thewalt, U. *Coord. Chem. Rev.* **2006**, *250*, 155 and references therein.
(20) Perrin, L.; Sarazin, Y.; Kirillov, E.; Carpentier, J.-F.; Maron, L. *Chem.−Eur. J.* **2009**, *15*, 3773.
(21) (a) Minieri, G.; Corradini, P.; Zambelli, A.; Guerra, G.; Cavallo, L. *Macromolecules* **2001**, *34*, 2459. (b) Minieri, G.; Corradini, P.; Guerra, G.; Zambelli, A.; Cavallo, L. *Macromolecules* **2001**, *34*, 5379.
(22) (a) Yang, S. H.; Huh, J.; Yang, J. S.; Jo, W. H. *Macromolecules* **2004**, *37*, 5741. (b) Yang, S. H.; Huh, J.; Jo, W. H. *Organometallics* **2006**, *25*, 1144.
(23) Usual average Eu−C(arene) bond lengths reported for complexes [(η^6−C_6Me_6)Eu($AlCl_4$)$_2$]$_4$ and [(η^6−C_6Me_6)Eu($AlCl_4$)$_2$]$_4$·($C_6H_2Me_4$) are of 2.999 Å: (a) Liang, H.; Shen, Q.; Jin, S.; Lin, Y. *J. Chem. Soc., Chem. Commun.* **1992**, 480. (b) Bochkarev, M. N. *Chem. Rev.* **2002**, *102*, 2089.
(24) (a) Kirillov, E.; Toupet, L.; Lehmann, C. W.; Razavi, A.; Kahlal, S.; Saillard, J.-Y.; Carpentier, J.-F. *Organometallics* **2003**, *22*, 4038. (b) Kirillov, E.; Toupet, L.; Lehmann, C. W.; Razavi, A.; Carpentier, J.-F. *Organometallics* **2003**, *22*, 4467. (c) Kirillov, E.; Saillard, J.-Y.; Carpentier, J.-F. *Coord. Chem. Rev.* **2005**, *249*, 1221.
(25) Bochmann, M.; Lancaster, S. J.; Hurthhouse, M. B.; Mazid, M. *Organometallics* **1993**, *12*, 4718.
(26) Kirillov, E.; Kahlal, S.; Roisnel, T.; Georgelin, T.; Saillard, J.-Y.; Carpentier, J.-F. *Organometallics* **2008**, *27*, 387.
(27) Alt, H. G.; Samuel, E. *Chem. Soc. Rev.* **1998**, *27*, 323.
(28) (a) Maron, L.; Eisenstein, O. *J. Am. Chem. Soc.* **2001**, *123*, 1036. (b) Maron, L.; Perrin, L.; Eisenstein, O. *Dalton Trans.* **2002**, 534.
(29) Andrae, D.; Haeussermann, U.; Dolg, M.; Stoll, H.; Preuss, H. *Theor. Chim. Acta* **1990**, *77*, 123.
(30) Hariharan, P. C.; Pople, J. A. *Theor. Chim. Acta* **1973**, *28*, 213.
(31) (a) Becke, A. D. *J. Chem. Phys.* **1993**, *98*, 5648. (b) Burke, K.; Perdew, J. P.; Wang, W. In *Electronic Density Functional Theory: Recent Progress and New Directions*; Dobson, J. F., Vignale, G., Das, M. P., Eds.; Plenum: New York, 1998.
(32) Frisch, M. J.; Trucks, G. W.; Schlegel, H. B.; Scuseria, G. E.; Robb, M. A.; Cheeseman, J. R.; Zakrzewski, V. G.; Montgomery, J. A.;

Stratman, R. E.; Burant, J. C.; Dapprich, S.; Millam, J. M.; Daniels, A. D.; Kudin, K. N.; Strain, M. C.; Farkas, O.; Tomasi, J.; Barone, V.; Cossi, M.; Cammi, R.; Mennucci, B.; Pomelli, C.; Adamo, C.; Clifford, S.; Ochterski, J.; Petersson, G. A.; Ayala, P. Y.; Cui, Q.; Morokuma, K.; Malick, D. K.; Rabuck, A. D.; Raghavachari, K.; Foresman, J. B.; Cioslowswi, J.; Ortiz, J. V.; Baboul, A. G.; Stefanov, B. B.; Liu, G.; Liashenko, A.; Piskorz, P.; Komaromi, I.; Gomperts, R.; Martin, R.; Fox, D. J.; Keith, T.; Al-Laham, M. A.; Peng, C. Y.; Nanayakkara, A.; Gonzalez, C.; Challacombe, M.; Gill, P. M. W.; Jonhson, B.; Chen, W.; Wong, M. W.; Andres, J. L.; Head-Gordon, M.; Replogle, E. S.; Pople, J. A. *Gaussian 03, Revision D-02*; Gaussian, Inc.: Pittsburgh PA, 2003.

(33) Reed, A. E.; Curtiss, L. A.; Weinhold, F. *Chem. Rev.* **1988**, *88*, 899.

(34) Clark, D. L.; Gordon, J. C.; Hay, P. J.; Martin, R. L.; Poli, R. *Organometallics* **2004**, *21*, 5000.